Self-organized patterns in successive bifurcations in planar semiconductor-gas-discharge device

Yu. A. Astrov,* A. N. Lodygin, and L. M. Portsel
Ioffe Institute, Politekhnicheskaya 26, St. Petersburg 194021, Russia
(Received 5 October 2014; revised manuscript received 11 February 2015; published 13 March 2015)

The formation of dissipative structures is investigated in a planar semiconductor-gas-discharge device at room temperature. The width of the discharge gap is about 1 mm. The gap is filled with nitrogen at a pressure that corresponds to the discharge operation at the right branch of the Paschen curve. Wafers of semi-insulating GaAs that exhibit linear transport in the whole range of voltage and current studied are used as semiconductor electrodes. In addition to the earlier investigated Andronov-Hopf bifurcation, a different mode of self-organization of the device is observed, where the transport of charge proceeds through an ensemble of pulsating current filaments. The corresponding critical current for the present bifurcation does not depend on the polarity of the bias voltage, while the spatiotemporal dynamics of a pattern differs substantially for a change in the polarity. Pulsating filaments can form a spatially ordered pattern when the GaAs electrode is under the positive potential. We also observe self-organization modes, where pulsating filaments form an irregular spatiotemporal dynamics of a pattern. The data obtained are briefly discussed in the frame of corresponding theoretical results in the field.

DOI: 10.1103/PhysRevE.91.032909 PACS number(s): 89.75.Kd, 52.80.Hc, 52.25.Gj, 52.35.Mw

I. INTRODUCTION

Gas discharge represents an extreme nonequilibrium system whose uniform steady state very often turns out to be unstable. As a result, various nonlinear phenomena leading to the appearance of temporal, spatial, and spatiotemporal dissipative structures (DSs) are observed in gas-discharge devices. Such self-organization phenomena occur, particularly, in planar gas-discharge structures where one of the electrodes is made of a semiconductor of high resistivity. In contrast to a device where both electrodes are fabricated from metal, a high-resistivity electrode has an inhibitory effect on the discharge processes in the gap. The gas-discharge region and the semiconductor electrode are specified by the different dynamics of the processes in them. The resulting interaction of the two coupled components of a whole structure may give rise to spatiotemporal behavior of DSs not observed in devices where both electrodes are made of metal.

A pioneering experimental study on the pattern-forming properties of semiconductor-gas-discharge (SGD) structures was performed by Purwins *et al.* (see the review article in Ref. [1]). The group investigated quasi-one-dimensional systems at the room temperature. One size of such a system, in the direction transverse to the current, was an order of the interelectrode distance. The length of the system in the other direction, normal to current, was much larger than the above dimensions. Electrodes made of high-resistivity silicon were implemented in the structures. Argon, helium, and mixtures of these gases with air were used to fill the discharge gap [2–5]. In the cited studies, a number of DSs were observed, among them stationary solitary current filaments and periodic (Turing-like) distributions in current and propagating structures. Also discovered was an interesting phenomenon in the behavior of DSs: spontaneous splitting of a solitary current filament [3]. Complicated spatiotemporal DSs were also observed in the studied systems, whose characteristics seemed to manifest the presence of spatiotemporal chaos in the dynamics of the discharge state [5].

In the cited works, the formation of spatial structures of current in the SGD structures was interpreted in terms of reaction-diffusion equations. The loss of stability of a spatially homogeneous state of the system was assumed in Refs. [2–5] to be related to the transition of the discharge to the glow mode. An experimental estimate of current in a formed filament [2] gives the value of $\sim$ 2 mA/filament, which is consistent with this interpretation. A general theoretical analysis of the problem as well as further references to experimental data can be found in Ref. [6].

Similar experiments were carried out using a planar SGD device equipped with an electrode made of high-resistivity semi-insulating gallium arsenide (GaAs) [7]. The study was done at room temperature; the discharge gap was filled with nitrogen. In accordance with the obtained data, a spatially uniform steady state of the discharge was observed at low current density $j < 0.1$ mA/cm^2. When the current reached a certain critical value, spatially homogeneous oscillations of current occurred in the device, i.e., the Andronov-Hopf bifurcation was observed. Images of the gas-discharge area recorded by a CCD camera that provided short exposure times, comparable to the period of oscillations, showed that oscillations occurred uniformly over the area of the gas-filled region.

Experiments carried out in Ref. [8] have demonstrated that a semiconductor electrode itself may be responsible for the loss of stability of the uniform stationary state of a planar gas-discharge device observed in Ref. [9]. The point is that the semiconductor component of a SGD structure normally operates at a high electric field inside it. This may activate a nonlinearity in the *I-V* characteristic of a semiconductor component of the hybrid structure. One such mechanism is the possibility of increased injection of nonequilibrium free carriers, either electrons or holes, depending on the polarity of voltage that biases the structure, from the gas-discharge plasma into the semiconductor volume. When injected carriers effectively modulate conductivity of the semiconductor volume, the *I-V* characteristic of the electrode becomes nonlinear (in

*yuri.astrov@mail.ioffe.ru

this case, superlinear), which may give rise to filamentation of current [10,11]. To provide stability to the semiconductor electrode that contacts operates in correlation with the gas discharge, the discussed injection effect has to be suppressed. This may be achieved by the presence of deep trapping centers in the semiconductor, whose density has to be high enough.

Another source of unstable operation of a SGD structure is the nonlinearity of a semiconductor electrode, which gives rise to the N shape of its *I-V* curve. This effect is well known to exist in some types of semi-insulating GaAs and is due to an increase in the recombination rate of nonequilibrium free carriers in the semiconductor at a high electric field (see, e.g., the review in Ref. [12]. Applying such an electrode in the SGD device may yield complicated spatiotemporal patterns when the voltage of the electrode reaches a critical value [13–15]. Essentially, some patterns observed in experimental study [9] have been self-organized in the semiconductor electrode, while the planar gas-discharge region just provided their visualization. Further study of the formation of spatial patterns within the ensemble of charge carriers in the laterally extended samples of semi-insulating GaAs is lacking. We may conclude, therefore, that the formation of spatially inhomogeneous DSs in SGD planar devices at the room temperature, which is caused by instability of the gas discharge, has not been unambiguously proved.

As follows from the above discussion, the transport characteristic of the semiconductor electrode is an important issue that has to be taken into account when studying pattern formation in a SGD structure. To study the phenomenon of self-organization of spatiotemporal DSs in the device initiated only by processes in the discharge, one has to apply electrodes whose conductivity does not depend on the device current and the voltage drop on the electrode. Exactly such a type of electrode that demonstrates linear *I-V* curves has been used both in the experimental investigation of the oscillatory instability of SGD systems in Refs. [16,17] and in the present study.

Instabilities in SGD devices for the case of discharge in nitrogen were analyzed theoretically in several publications [18–22]. As a cause of the observed effect at relatively low currents, a strong dependence of the secondary electron emission coefficient on the discharge current density was assumed in Ref. [21]. Taking into consideration this effect when analyzing the stability of gas discharge goes back to earlier theoretical works [23,24] on the subject.

In the study of Šijačić and co-workers [18–20], the origin of oscillatory instability in the devices has been considered to be related to the effect of the ion space charge in the discharge gap on the avalanche multiplication of free electrons there. However, a detailed comparison of the experimentally observed critical current density j_{cr} [17] with theoretical estimates performed in Ref. [19] reveals that measured j_{cr} are essentially lower than theoretical values. So the effect of the ion space charge is not strong enough to explain the experimental data. Therefore, we have interpreted small values of j_{cr} observed in Ref. [17] by taking into account the possible dependence of secondary electron emission on the discharge current [21].

One of the important conclusions of theory [18,20] is that the oscillating homogeneous state may be also unstable with respect to patterning of the discharge in the direction transversal to the current. Such a spatiotemporal (Turing-Hopf) mode may have the form of weak running waves of a long wavelength. We point out that waves running in the transverse direction, similar to those that would be expected on the basis of theoretical analysis [18,20], were observed in the SGD structures investigated in Refs. [8,14]. However, since GaAs electrodes used in these experiments had pronounced nonlinear properties, the data could not be regarded as an experimental proof of the existence of such a phenomenon at the expense of the active role of gas discharge (see also [15]). We can conclude, therefore, that there has been no experimental observation of the above-discussed scenario of self-organization of SGD devices, which could be due to the active role of gas discharge.

In this paper, we investigate the discharge dynamics in the planar SGD system at room temperature. The main body of the study is done by filling the discharge gap with nitrogen. The paper is an extension of Ref. [17], where the spontaneous dynamics of the system in the stability domain and the transition to macroscopic oscillations at a critical current density (we refer to it here as j_{cr}^1) have been investigated. We stress that, similarly to experiments [7,8,16], relatively small values of j_{cr}^1 were observed in Ref. [17]: For example, at the gap width $d_g = 1.27$ mm and gas pressure $p = 30$ hPa, they were in the range of $j = 6$–100 μA/cm^2 (depending on the semiconductor electrode resistance R_S). This fact enables an experimental study of properties of the self-organizing system at nominally direct currents, which are substantially above j_{cr}^1. According to the obtained data, in addition to the earlier investigated Andronov-Hopf bifurcation [7,16,17], the formation of new self-organized DSs has been documented, which demonstrate strong localization of current. The dynamics of some patterns is quite irregular in time and space. At a certain state of the device, its overall current flows via an ensemble of oscillating current filaments. At a relatively high current density, the filaments can organize a spatially ordered pattern.

The amplitude of current density in an isolated pulsing filament is estimated by means of an image-processing technique. The obtained data allow us to conclude that the transition from Townsend to the glow discharge is responsible for the formation of the observed complicated DSs. Such transition events proceed at phases of the oscillation process where the active current reaches maximum density, which initiates a temporary breakthrough of the gap. For large amplitude of the spatially homogeneous oscillations, such a phenomenon may occur at a rather low time-averaged current in the device.

The phenomenon of loss of stability of the homogeneously oscillating state of the studied system in general corroborates the conclusions from theoretical results [18,20]. The observation of irregular spatiotemporal dynamics of the device, where patterns are formed by pulsating current filaments, is in qualitative correspondence with the mode of current patterning in a one-dimensional (1D) SGD structure, which has been demonstrated recently in numeric modeling of discharge processes there [22].

Some experiments aimed to observe similar effects by filling the discharge gap with Ar are also made in the current study. The fixed parameters of the discharge gap (p and d_g) have been close to those implemented in experiments with

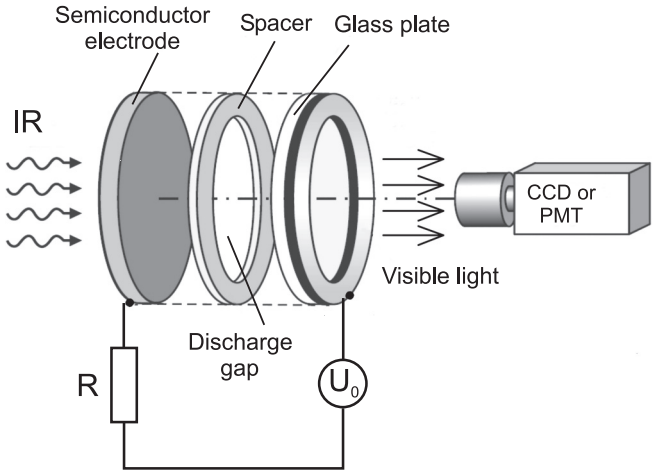

FIG. 1. Schematic presentation of the experimental setup. The diameter of the discharge area is 15 mm. A photomultiplier tube (PMT) and different CCD cameras are used to investigate the discharge dynamics. For further experimental details, see [17].

N_2. However, no peculiarities in the discharge dynamics are revealed in this case.

II. EXPERIMENTAL SETUP

The experimental setup is essentially the same as that implemented in a set of earlier studies, e.g., [7,14,17]. The investigated gas-discharge device is a parallel-plane structure, the two main components of which are a semiconductor wafer and a gas-discharge gap (Fig. 1). The wafer is fabricated from photosensitive semi-insulating GaAs and serves as a high-resistivity electrode to the discharge gap. One of the electrical contacts to the structure is a metallic (Ni) thin film deposited on the outer surface of the wafer. It is transparent to the IR light, which permits one to control the resistivity of the GaAs electrode optically, with an IR light source. In the experiments, we used electrodes that exhibit linear *I-V* characteristics in the whole ranges of applied voltage and intensity of illumination.

The width of the discharge gap and its extension in the lateral dimension are defined by a dielectric spacer, which has a round opening in the center. The other electrode of the device is transparent to the visible light. It is a glass plate covered with a high-conductivity SnO_2 layer. The discharge gap of width d_g is filled with nitrogen whose purity is 99.97%. For additional purification of nitrogen from possible contaminants such as oxygen and water vapor before filling the system, gas is passed through a trap cooled with liquid nitrogen. Stanford Research Systems PS 325 serves as a high-voltage stabilized dc power supply. Electric current of the device is measured by the voltage drop on a monitor resistor.

The design of the SGD structure permits one to observe the spatial distribution of discharge glow in the gap. Different CCD cameras are applied in the present experiments for this purpose: Pieper FK, PCO Sensikam QE, and Phantom, model v1610. The first camera allows one to take single pictures of the discharge area with the exposure time $\tau_{exp} = 20$ ms and also to make movies at the video frequency. A camera PCO Sensikam can be used to record images of a different τ_{exp}, down to the shortest value of 0.5 μs. The rate of taking images with this camera does not exceed 1 frame/s in our experiments. The high-speed Phantom camera has been applied in one experiment. According to the data obtained, this camera is able to perform imaging of the discharge area of our setup with a speed of up to 3×10^5 frames/s. However, such a speed could be reached only for the filamentary mode of discharge, where a strong localization of current is observed. To study the global dynamics of discharge, a photomultiplier tube (PMT) is used to record the time series of the integral discharge glow by the oscilloscope LeCroy 7300A.

The present study is carried out at room temperature. Both polarities of voltage applied to the device's electrodes are used. The main body of the study is done at $d_g = 0.84$ mm and $p = 4.15$ mmHg or, in SI units, at $p = 66$ hPa, which corresponds to the right branch of the Paschen curve (product $pd_g = 5.54$ hPa cm). The typical diameter of the discharge channel is 15 mm. This set of parameters is close to that investigated in experimental works [7,13,17] and implemented in the theoretical description of self-organization of the SGD systems [18–22]. Some measurements are made for the gap width $d_g = 0.11$ mm and pressure $p = 100$ hPa, which is near the minimum of the Paschen curve. In addition to the experiments carried out by filling the gap with N_2, a preliminary study of the device with Ar filling is performed.

III. EXPERIMENTAL RESULTS

Figure 2 shows the global current-voltage (*I-V*) curves of the SGD system measured for two sets of parameters of the

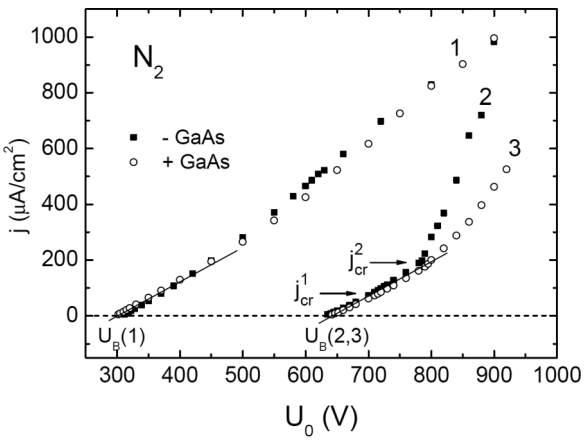

FIG. 2. The *I-V* curves of the SGD structure measured for both polarities of the applied voltage for two sets of parameters of the discharge gap. The resistance R_S of the GaAs electrode is 7.3×10^5 Ω. Curve 1 is obtained for the gap width $d_g = 110$ μm and $pd_g = 1.10$ cm hPa. Curves 2 and 3 refer to the right branch of the Paschen curve: $d_g = 0.84$ mm and $pd_g = 5.54$ cm hPa. Two subsequent bifurcations of the device state are observed for these parameters of the gap. They are marked with arrows (see the text). The corresponding critical current densities are $j_{cr}^1 \approx 80$ μA/cm^2 and $j_{cr}^2 \approx 190$ μA/cm^2. Straight lines that interpolate experimental points at low currents are inclined at the same angle relative to the abscissa axis of the plot. This indicates equal differential resistance of the structure at low current in both experiments.

discharge gap. The data are obtained at some fixed value of resistance of the GaAs electrode, which is $R_S = 7.3 \times 10^5\ \Omega$. ($R_S$ is defined for 1 cm^2 of the structure aperture. The current density is current per unit discharge area.) The data used to obtain curve 1 in the figure refer to the gap width $d_g = 110\ \mu$m and $p = 102$ hPa. At these parameters, the product pd_g (1.10 cm hPa) is close to the minimum of the Paschen curve for nitrogen [25]. Curves 2 and 3 are measured for $d_g = 0.84$ mm and $pd_g = 5.54$ cm hPa, which correspond to the right branch of the Paschen curve.

One can see a remarkable difference in the *I-V* characteristics of Fig. 2. The dependence (1) is practically linear in the whole range of applied voltage. The slope of the curve (that is, the derivative $\partial U/\partial j$) equals the electrode resistance R_S. We note that the *I-V* curves almost coincide for the two polarities of the bias voltage at the given values of p and d_g.

In the case of $d_g = 0.84$ mm, the linearity of the *I-V* characteristics is observed only in the range of relatively low current density $j < 200\ \mu$A/cm^2. At a higher current, a significant change in the slope of the characteristics can be seen. Moreover, the curves exhibit a difference for the two polarities of applied voltage: When the semiconductor serves as an anode, the slope of the *I-V* curve is significantly increased compared to the case of opposite polarity.

Since we use electrodes that have linear transport properties, the linearity of the *I-V* curve 1 in the whole studied range of current, as well as of characteristics (curves 2 and 3) for currents not exceeding ~200 μA/cm^2, means that the discharge sustaining voltage remains almost constant there regardless of the current. Therefore, one may conclude that we deal in both cases with the Townsend type of discharge. Nevertheless, experiments show that an oscillatory *instability* inside the range of Townsend discharge may be observed, which is the Andronov-Hopf bifurcation. That is, the discharge remains stable only in some range of current that is narrower than the range of existence of the Townsend discharge [17]. The value of the critical current j_{cr}^1 for this instability (see below) is marked on the *I-V* curves 2 and 3 of Fig. 2. We stress also that for the *I-V* characteristic 1 in the figure, the system remains stable in the whole range of current.

To specify the variation of global features of discharge dynamics in planar SGD systems while changing the current, we have used in Ref. [17] a parameter related to the power of oscillatory components of discharge. Such a parameter was introduced there as an integral of components $A(f)$ of a Fourier spectrum

$$\widetilde{P}(\triangle f) \propto \int_{f_0}^{f_1} A(f)df$$

of a time series of the discharge glow intensity $E(t)$ recorded with the PMT (see Fig. 1). As in Ref. [17], we define the parameter $\widetilde{P}(\triangle f)$ in the frequency range (5×10^3)–(2×10^6) Hz.

Plotting $\widetilde{P}(\triangle f)$ as a function of the time-averaged current density allows us to determine critical currents at which the discharge dynamics changes qualitatively; see Fig. 3, where a sharp increase in the $\widetilde{P}(\triangle f)$ values at the points of bifurcation is characterized by inflection points on the curves. The critical current $j_{cr}^1 \approx 80\ \mu$A/cm^2 corresponds to spontaneous generation of spatially homogeneous oscillations of the discharge current, that is, the Andronov-Hopf bifurcation is observed. Note that j_{cr}^1 values practically coincide for both polarities of the applied voltage. We also note that the $\widetilde{P}(\triangle f)$ value is proportional to $j^{0.5}$ at $j < j_{cr}^1$, which is characteristic of the stable state [17].

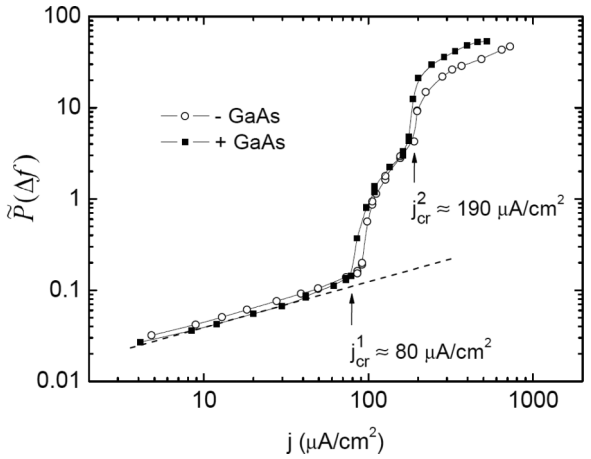

FIG. 3. Dependences of power of the oscillatory components in the discharge dynamics on current density. Results refer to the conditions of obtaining the *I-V* curves of Fig. 2 for the gap width 0.84 mm. The arrows mark critical current densities for two bifurcations in the device's state (see the text). For the stable state of the structure, a $j^{0.5}$ dependence of oscillatory power on current density is observed (shown with the dotted line).

Other inflection points on curves 2 and 3 in Fig. 3 give an indication of the next change in the dynamics of the device. We refer to the corresponding critical currents as j_{cr}^2. These bifurcations are observed (similarly to those at j_{cr}^1) at practically equal currents for both polarities of applied voltage. However, at $j > j_{cr}^2$ one can see that the oscillatory power of the device is essentially higher at the polarity where the semiconductor electrode serves as an anode.

Some specific features of discharge dynamics for different values of global current density, that is, of j values obtained by averaging the current in time and over the square of the planar structure, are illustrated by the data in Figs. 4 and 5. These results refer to the polarity of applied voltage

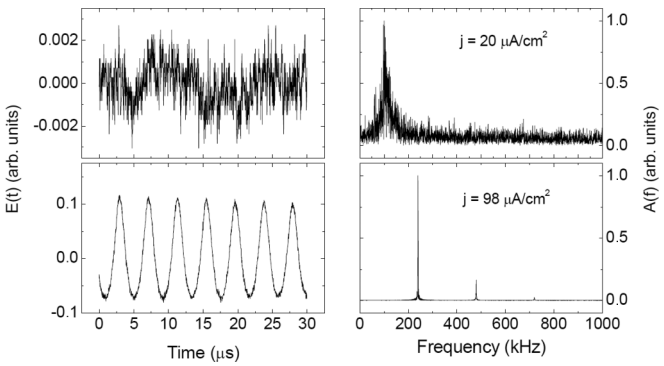

FIG. 4. Typical time series of the discharge glow and Fourier spectra at current densities below and above j_{cr}^1. Data correspond to the *I-V* curves observed at $d_g = 0.84$ mm (Figs. 2 and 3).

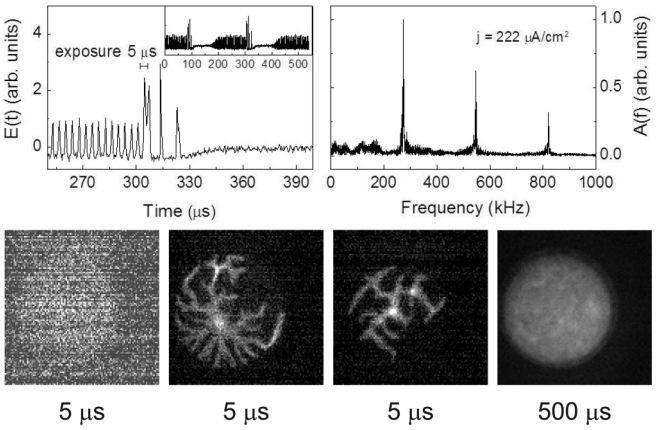

FIG. 5. Features in discharge dynamics observed at the current density 222 μA/cm^2, which is somewhat higher than j_{cr}^2 (see Figs. 2 and 3). The GaAs electrode serves as a cathode. The diameter of the discharge cell is 15 mm. Shown on the top is an example of time series of the discharge glow, given at two time scales, and the corresponding Fourier spectrum. Typical images of the discharge are obtained at random times at a long and short τ_{exp} (see the text).

where the semiconductor electrode serves as a cathode. The data shown in Fig. 4 present examples of oscilloscopic traces $E(t)$ and the corresponding amplitude-frequency spectra $A(f)$ of the discharge glow observed at the current density $j = 20$ μA/cm^2 $< j_{cr}^1$ (that is, at a stable steady-state of the device) and at a current that is somewhat higher than j_{cr}^1 ($j = 98$ μA/cm^2). The spectra are the modulus of the Fourier transform $A(f)$ of corresponding time series for the discharge glow. In the stable state of the device, discharge noise is observed in broadband frequencies and is characterized by a maximum at some frequency f_0. According to the results of Ref. [17], the f_0 value increases with current density as $j^{0.5}$. At an increased current, at $j = 98$ μA/cm^2 for the data presented in Fig. 4, weakly nonlinear oscillations in the discharge glow can be seen; the amplitude-frequency spectrum of the gas glow contains now a strong component at ≈240 kHz.

For a current exceeding j_{cr}^2 (in Fig. 5, data refer to $j =$ 222 μA/cm^2), a more complicated dynamics of the device is observed. The left graph in the upper part of the figure depicts the observed dynamics at two time scales. The long-time observation (inset in the graph where a fragment of a time series recorded during 600 μs is shown) demonstrates that the dynamics, while being quite complicated, has signs of some regularity: A sequence of a small number of large-amplitude pulses is followed by the discharge decay. Then a slow increase in the discharge brightness with no oscillations is observed. At some stage of this process, regular oscillations appear and exist for a rather long time, which is about 100 μs in the case shown. Finally, the oscillations induce a few successive current spikes that are followed by the discharge termination and the process repeats, more or less cyclically. The overall variation of the signal in time is reminiscent of the so-called intermittency effect observed in many nonlinear systems. Such behavior of a dynamical system is known to be among the canonical routes to chaos (see. e.g., [26]).

We note also that the Fourier spectrum of the device's dynamics (Fig. 5) contains the main and higher harmonics. These reflect extended temporal patches of almost periodic oscillations in the time series of the signal. Disorder in the spectrum seen mainly at relatively low frequencies is related to disturbances in periodicity of the signal.

The informative data on discharge dynamics at a relatively high global current are revealed by taking images of the discharge at different τ_{exp}. The pictures in Fig. 5 are recorded by a Sensikam camera with $\tau_{exp} = 5$ and 500 μs. Images taken at short τ_{exp} in general manifest fairly complicated discharge patterns (see images in Fig. 5 recorded at $\tau_{exp} = 5$ μs). These pictures demonstrate the existence of well-localized discharge channels (or solitary current filaments) on a short-time scale, which are connected to branching (fractal-like) patterns. The scale of an exposure time of 5 μs is marked on the time series of the figure by the horizontal bar. It can be seen that such an exposure time is of the order of a duration of one or two high-amplitude pulses in the time series. So the appearance of filaments or discharge patches in the gap seems to be connected to the formation of such pulses. We point out that there exist stages in the discharge where it is characterized by a faint spatially homogeneous glow (see the leftmost picture in Fig. 5). It can also be observed that images taken at a long exposure time reveal almost uniform in space discharge glow (see the example shown in the rightmost picture in Fig. 5 taken at $\tau_{exp} = 500$ μs). This allows us to conclude that flashing filaments fill up the discharge space homogeneously in the course of time.

It is found that pattern formation in the device differs substantially with changing polarity of the bias voltage, with other conditions being similar. An example of data for the polarity where the semiconductor electrode serves as an anode is shown in Fig. 6. It presents an oscilloscopic trace of the discharge glow, the corresponding Fourier spectrum, and images of the gas-discharge region; all results refer to $j = 288$ μA/cm^2, that is, to current exceeding j_{cr}^2. The data in the figure are organized in the same way as in Fig. 5. At this polarity, oscilloscopic traces demonstrate the patterns of spike bursts occurring more or less periodically in time (see the example in the figure). Short exposures now make

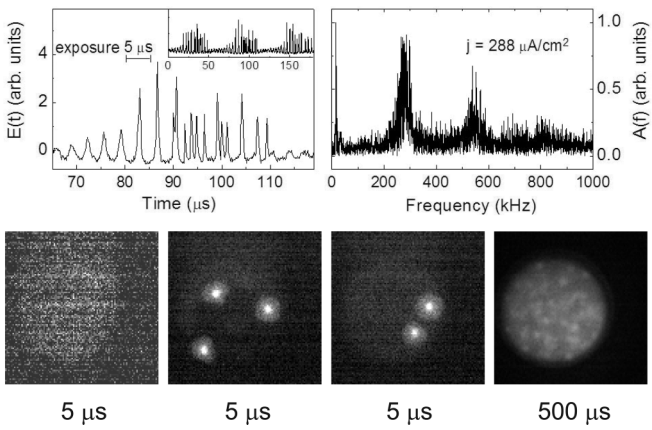

FIG. 6. Data similar to those presented in Fig. 5, but obtained at the polarity of applied voltage where the semiconductor electrode serves as an anode. The fixed parameters of the discharge gap are the same as those used to get the results of Fig. 5.

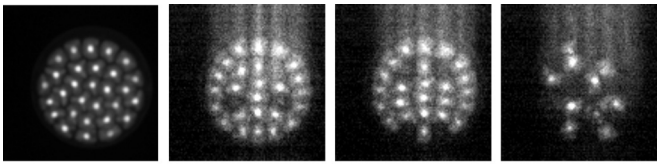

FIG. 7. Examples of patterns in the device observed at $j = 1.17$ mA/cm^2 and different τ_{exp} (see the text). The semiconductor electrode is under the positive potential. The fixed parameters of the discharge gap are the same as those used to get the data of Figs. 5 and 6. Vertical bands in pictures observed at short τ_{exp} are due to the specifics of the operation of the CCD camera sensor.

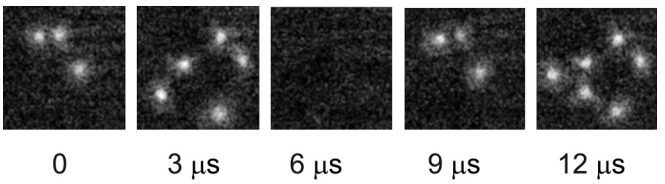

FIG. 8. Sequence of images obtained by the high-speed Phantom camera at the rate of 3×10^5 frames/s. The parameters of the SGD structure and other experimental conditions are similar to those used to get the data of Fig. 7.

visualization of solitary filaments possible: Corresponding images in the figure contain two and three filaments, while fractal-like patterns are not observed. As for the leftmost picture in the figure, it seems to be the result of recording the device's state between bursts of spikes, which represents a spatially homogeneous and faint glow.

In the rightmost image in Fig. 6, which is obtained at a relatively long $\tau_{exp} = 500$ μs, the discharge appears again, as we have seen at a close value of current for the other polarity, as a spatially homogeneous object. After having compared the pictures of discharge at short and long exposure times, we may again conclude that flashing filaments fill up the discharge space homogeneously in the course of time.

It has been found that the spatial distribution of current filaments in the discharge region can evolve into a rather regular spatial structure. This is observed at a relatively high current density in the polarity where the semiconductor electrode is under a positive potential. Such a DS can be seen in the leftmost picture of Fig. 7. The image presents a snapshot of the discharge state recorded at $\tau_{exp} = 415$ μs for the averaged current density $j = 1.17$ mA/cm^2. The pattern represents a hexagonal structure with fixed spatial positions of elements.

However, at shorter τ_{exp} a complicated dynamics of the pattern is also revealed in this case. It is observed that filaments that form the structure do not appear in the gap simultaneously. One can see that the images obtained at $\tau_{exp} = 5$ μs contain fewer elements than those obtained at long τ_{exp}. For example, an ordered structure recorded at $\tau_{exp} = 415$ μs consists of 29 filaments. Two images recorded at $\tau_{exp} = 5$ μs have a few elements missing: They contain only 25 and 24 elements, respectively. In the snapshot of the dynamics obtained at $\tau_{exp} = 2$ μs, only 9 elements of 29 exhibited at $\tau_{exp} = 415$ μs are present. As can be seen in the set of images of Fig. 7, the position of pulsating current filaments is fixed in the discharge gap space (they are spatially trapped in the case studied). We note, however, that a change can also be observed in the configuration of the pattern at a long time of observation: For example, a turn of the whole pattern at some angle may spontaneously occur, while the pattern keeps hexagonal symmetry.

We have to stress that the experimental setup used to get the images shown in Figs. 5 and 6 could facilitate acquisition of images only at a rather low repetition rate (typically, less than 1 frame/s). In experiments, there has been no possibility of synchronizing the exposure time to a phase of the physical process. Therefore, pictures obtained at the short τ_{exp} and shown in the above figures have been taken in a random way and present exemplary phases of the system's dynamics.

Supposing that the intensity of light emission from gas in the gap is proportional to the discharge current, it is possible to estimate the current density in pulsating filaments j_{fil} from a recorded image of a pattern. To obtain such data, the Sensikam camera has been calibrated with the purpose to establish, at a given exposure time, the relation of the number of counts in a signal of an image to the discharge current density. Such a calibration has been performed at $j < j_{cr}^1$, that is, at a spatially homogeneous and steady-state discharge.

Making the calibration of the image acquisition equipment and then processing an image like that shown in Fig. 7 gives $j_{fil} \approx 4$ mA/cm^2. Apparently, this estimate gives only an approximate value of the current density in a filament because the duration of exposing the camera sensor by a flashing filament is not precisely known in our experiments: If the filament lifetime is less than the camera exposure time (which is 5 μs in the case considered), then the applied method underestimates the j_{fil} value.

According to a straightforward estimate based on a conventional model of the Townsend discharge [25], the above value of instantaneous j_{fil} substantially exceeds the current density at which, at given parameters of the discharge gap, space charge phenomena inherent to the glow mode of discharge have to be observed in a current filament. We can conclude, therefore, that it is the transition from the Townsend to the glow discharge that initiates the formation of flashing current filaments in the gap: At such a transition, voltage sustaining a discharge is known to decrease with an increase in the concentration of charge carriers in the gap, which provides the negative differential resistance (NDR) of the discharge region and facilitates the instability.

Supplementary data on the dynamics of patterns are obtained while applying the high-speed camera Phantom v1610. It is demonstrated that the camera can record images of the discharge at a speed of up to $\sim 3 \times 10^5$ frames/s. However, this has become possible only for the filamentary mode of discharge in the device. A sequence of snapshots recorded at such speed is presented in Fig. 8. Only part of the discharge aperture has been captured by the lens of the camera in this experiment. The data refer to the polarity of the bias voltage where the GaAs electrode is an anode. The parameters of the SGD device and the time-averaged current density are close to those used to get the data shown in Fig. 7.

It is shown that subsequent frames may demonstrate quite different spatial forms of discharge patterns. However, while

investigating a sequence of snapshots, the tendency of recovery of a discharge state observed at an earlier stage of dynamical process is revealed. In particular, such regularity in the dynamics can be seen when comparing the images of Fig. 8 taken at 0 and 9 μs. One can assume that it is this effect that is responsible for the observation of a seemingly regular spatial pattern like the one presented in Fig. 7 at $\tau_{exp} = 415$ μs. We add to the point that a procedure of accumulation of pictures belonging to a sequence like that shown in Fig. 8 produces a spatially ordered pattern. We stress that for the opposite polarity of the applied voltage, where the semiconductor electrode serves as the cathode, different behavior of the dynamical system is observed. Now, the ergodicity of the device's dynamics is maintained even at a relatively high current density corresponding to that used to obtain the data of Fig. 7.

A relatively low bifurcation value of j_{cr}^2 for the filamentation process (see Figs. 2 and 3) seems to be related to features of the oscillatory state of the system for which the new instability is observed. An increase in global current density in the range $j > j_{cr}^1$ is accompanied by growth of the peak-to-peak values of discharge oscillations. This results in a high current density during the phase of the oscillation process, where the current is maximal. Note that the observed frequencies of current oscillation in the vicinity of the critical state j_{cr}^1 are relatively low and do not exceed several hundred kHz, which is much less than the inverse time of flight of charge carriers through the gap. Therefore, one can assume that the structure of the ion space charge in the gap is self-consistently coupled to the local current density. In other words, the spatial distribution of free charges in the gap for a stage of the oscillatory process at a given instantaneous current is essentially the same as for a steady-state discharge at the same current density.

When the oscillation amplitude reaches some critical value, an instantaneous current becomes large enough for a transition to the glow discharge to occur, which can generate a local current filament. Such an interpretation of the filamentation process is supported by the observation of the dynamics of the discharge at (or near) the bifurcation point. An example of a corresponding time series of the discharge signal recorded by the PMT is presented in Fig. 9. The experiment shows

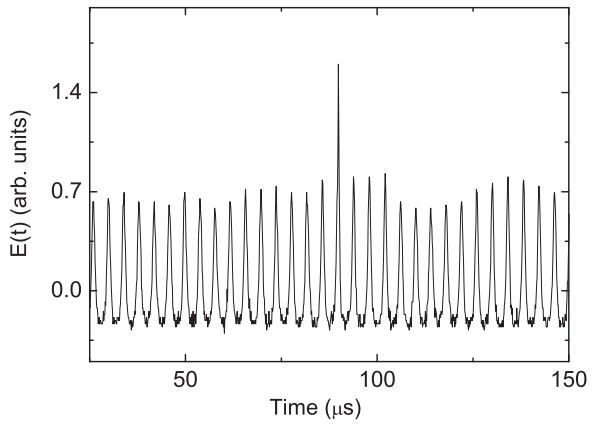

FIG. 9. Example of time series of the discharge glow in the vicinity of the critical state j_{cr}^2. The semiconductor electrode is under the positive potential.

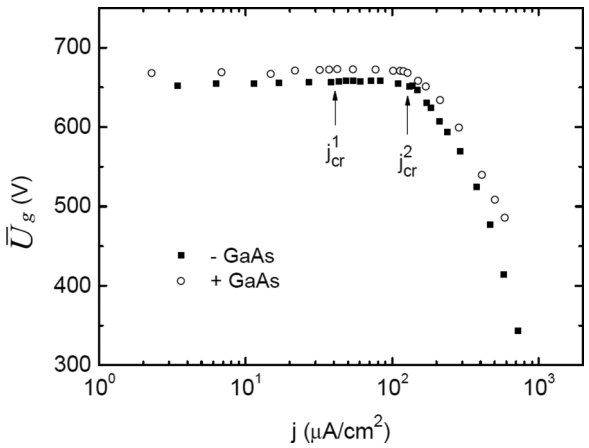

FIG. 10. Time-averaged *I-V* curves of the discharge gap. The results refer to the same fixed parameters of the discharge gap as those used to obtain the data of Fig. 2. For details of the calculations of the curves, see the text.

that breakthroughs appear in the discharge glow that occur on the background of more or less regular oscillations. When increasing the device current further, such breakthroughs become more and more frequent. For the developed process, that is, far from the bifurcation point j_{cr}^2, the dynamics become very complicated [see time series $E(t)$ in Fig. 6].

An indication of the significant role of effects that are characteristic of the glow discharge in the device can be seen in the dependences shown in Fig. 10. This graph represents the average voltage on the gap $\overline{U}_g$ as a function of the average current density $\bar{j}$. Here $\overline{U}_g$ values are calculated by subtracting the voltage drop on the semiconductor electrode (determined as the product $\bar{j}R_S$) from the supply voltage U_0. Such a procedure is applicable because the electrode resistance remains constant at different currents. We stress, however, that the corresponding branches of the *I-V* curves 2 and 3 in Fig. 2, used to obtain the data of Fig. 10, are measured in the discharge oscillation mode and describe the relationship between the time-averaged values of current and voltage. So these are related to some global behavior of discharge in the structure, which reflects the complex spatiotemporal dynamics of current there.

It is shown that up to $\bar{j} = j_{cr}^2$ [which is $\approx$190 μA/cm^2 (see Figs. 2 and 3)], the discharge voltage is practically independent of the current. When the current density (averaged in time) exceeds j_{cr}^2, a decrease in the $\overline{U}_g$ values is observed with an increase in the current, i.e., a NDR of the discharge region appears. We point out that the NDR of the discharge gap determined in this way refers to a dc regime, that is, it is related to electrical properties of the discharge region at frequency $f \approx 0$: The effect is the outcome of the complicated dynamics of DSs in the device. At some chosen voltage value, the current averaged in time depends on the voltage polarity: It is higher when the semiconductor electrode serves as a cathode.

Finally, we point out that the preliminary experimental data obtained by filling the discharge gap of the SGD device with argon, in the same range of current and parameters of the structure as in the case of nitrogen, do not show instabilities and the formation of patterns discussed above. We see, therefore,

that the stability of discharge in Ar at the right branch of the Paschen curve, as compared to N_2, is essentially increased.

IV. DISCUSSION AND CONCLUSIONS

In the present work, we have investigated the dynamics of a dc-driven planar semiconductor-gas-discharge device at room temperature and the formation of DSs there. The discharge gap of the device was filled with nitrogen; semi-insulating GaAs was used to fabricate semiconductor electrodes implemented in the experimental structure. To exclude the possible influence of nonlinear properties of a semiconductor on self-organization of DSs in the device, we applied electrodes that have linear *I-V* characteristics. The experiments were carried out at a discharge gap width of 0.84 mm, while the value of the pd_g product was ≈5.54 cm hPa. This corresponds to the right-hand branch of the Paschen curve. The dynamics of the system was investigated in an extended range of current density, up to ≈1.2 mA/cm^2, which allowed us to observe a number of self-organization phenomena in the device. Some of the DSs have not been previously documented. Among the present results is the observation of DSs composed of an ensemble of pulsed current filaments. These (or more complicated) spatially localized building elements of a DS may construct a pattern whose dynamics is quite irregular. At a large current density, DSs that consist of spatially ordered ensembles of pulsing current filaments were observed. This occurred at the polarity of the bias voltage where the semiconductor electrode serves as the anode.

In general, increasing the applied voltage U_0 while keeping the electrode resistance unchanged, the following sequence of bifurcations in the device can be considered.

(i) In the range $0 < U_0 < U_B$, where U_B is the gap breakdown voltage, there is no current in the structure. The voltage U_B is critical for the transition of the device to the conductive state. Increasing U_0 further is accompanied by the linear ($\partial U/\partial j = 1/R_S = \text{const}$) growth of current. A spatially homogeneous stationary discharge is observed at a low current.

(ii) At a current increase up to a critical value j^1_{cr}, the bifurcation to spatially homogeneous oscillations of current takes place. This phenomenon, the Andronov-Hopf bifurcation, has been observed in Ref. [7] and further studied in experimental works [9,16,17]. It has been established in Ref. [17] (see also data of Fig. 10) that bifurcation occurs inside the range of Townsend discharge in the gap: The global *I-V* characteristic of the device does not manifest features at the point of this bifurcation and remains linear in its vicinity. Correspondingly, the time-averaged voltage on the gap remains close to the breakdown value U_B. According to our results obtained in Ref. [17], the instability occurs at a current density much lower than that required for the transition from the Townsend to the glow discharge (which is generally considered as a cause of instability of low-current discharges). The destabilization of the device's state inside the domain of existence of the Townsend discharge can be interpreted when exploiting the hypothesis that the coefficient of secondary emission of electrons from the cathode may be dependent on the current or electric field near the cathode [21,23,24].

(iii) In the present study, we have found that the next critical state, at j^2_{cr}, is reached with a further increase in current. At this critical point, the transition to a spatially inhomogeneous oscillating state occurs. In the theoretical investigation of the dynamics of SGD structures [18,20], this change in dynamics is referred to as the Turing-Hopf bifurcation. Our study of the SGD structure reveals a variety of spatiotemporal DSs at $j > j^2_{\text{cr}}$.

The bifurcation is observed for both polarities of the bias voltage and is accompanied by a change in the slope of global *I-V* curves of the device at the discussed critical points. In contrast to the bifurcation at j^1_{cr}, now a different behavior of the system is observed for the two polarities of the bias voltage, its impedance being higher when the semiconductor electrode serves as the cathode (Fig. 2).

We have attempted to study the dynamics of DSs at $j > j^2_{\text{cr}}$ by implementing an image acquisition technique that is capable of taking pictures of the discharge area at different exposure times τ_{exp}. By applying the method at short τ_{exp} (in the range 2–5 μs), it has been found that spatial forms of DSs differ for the two polarities of applied voltage. If the semiconductor electrode serves as a cathode, flashing localized fractal-like patches are observed, whereas the DSs consist of flashing filaments for the reverse polarity of the bias voltage.

It is known that self-organization of a nonlinear system can lead to its chaotic behavior (see. e.g., the reviews in Refs. [27,28], where corresponding references can be found). In this regard, the question arises whether the irregular discharge dynamics observed in our experiments indicates the existence of chaos in the device. Up to now, the chaos theory has been developed primarily for lump systems and in this way operates with so-called temporal chaos. The problem of describing chaos in extended media is much more complicated (see the review in Ref. [27]). In the frame of the present study, we could analyze device dynamics only in terms of the emergence of the temporal chaos, i.e., chaos that can be detected in the analysis of temporal series of global variables of the dynamic system, in this case, the discharge glow that is recorded by the photomultiplier.

One parameter that can be used to determine whether the dynamic chaos is realized in a system is the Lyapunov exponent: Its positive value is the signature of chaos. In trying to reveal whether this can occur in the device, we have investigated time series of the discharge dynamics where it is quite irregular, for the average current density exceeding j^2_{cr}. As a mathematical tool, the software package TISEAN [29] is used. The program calculates a divergence rate of system trajectories in reconstructed phase space. For this, the average distance d between two nearest-neighbor trajectories in the phase space is computed as a function of time. Then the Lyapunov exponent can be found from the slope of the linear region of the graph $\ln d(t)$: When it is positive, one can claim the existence of the chaotic mode in the system [30,31].

Figure 11 presents an example of obtained $\ln d(t)$ dependences. The data are calculated for the time series shown in Fig. 5 (as pointed out above, such a curve may indicate the intermittency effect, which is known to be among the scenarios of the transition to chaos). The sampling rate to obtain the experimental curve is 5×10^7 s^{-1}. When making the calculation, we have followed the approach of analyzing

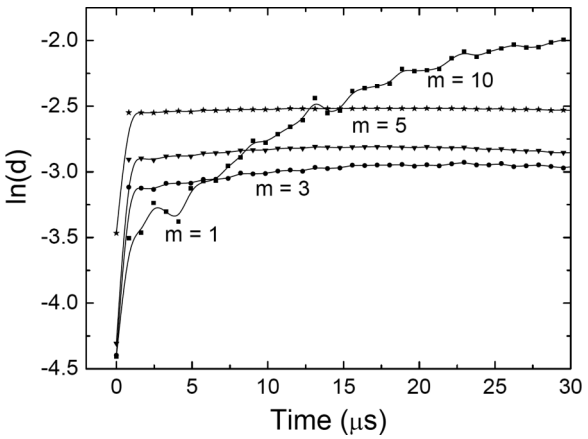

FIG. 11. Rate of divergence of trajectories in the reconstructed phase space for the discharge time series shown in Fig. 5. Curves approximate computed data (shown by points) and data obtained at different embedding dimensions m. For details, see the text.

a system's dynamics described in Refs. [30,31]. Results are obtained while using the reconstruction delay time $\tau = 8 \times 10^{-7}$ s and a set of embedding dimensions $m = 1, 3, 5$ and 10. The value of τ was determined from the autocorrelation function of the recorded variable as the time when it drops to $1 - 1/e$ of its initial value.

The obtained ln $d(t)$ dependences of Fig. 11 do not have a linear part whose slope could be associated with the exponential divergence of system trajectories in the phase space. (For further details of data processing and interpreting results, see [31].) We have to conclude, therefore, that the global dynamics of the device is not chaotic.

Still, one may ask whether, despite the absence of temporal chaos, the spatiotemporal mode of chaos may exist, where pulsating filaments in the effectively two-dimensional space of the device are created and destroyed not stochastically but by obeying some regularities specific for the chaotic process. However, it is not possible at present to answer this question.

The results of high-speed photography (Fig. 6) show that short-lived current filaments are generated in the course of time in such a way that they occupy the discharge gap more or less spatially uniformly. Such patterns' dynamics is accompanied by the irregular temporal behavior of the global discharge glow. We stress that the data of this figure refer to a relatively small number of filaments in the gap at each time point. These observations may indicate that the overall dynamic of the device is determined by stochastic generation of pulsed current filaments in space.

(iv) At relatively large current densities on the order of 1 mA/cm^2, there appears another difference between the spatiotemporal behaviors of the device for the two polarities of the bias voltage. Such data are again obtained by photographing the discharge region at both short and relatively long exposures. For the polarity where the semiconductor electrode is a cathode, the overall behavior of a DS is similar to that recorded at a lower j (but exceeding j_{cr}^2): An irregular spatiotemporal dynamics is observed, which is organized by flashing patches of discharge.

At the opposite polarity (where the semiconductor is an anode), implementing a long exposure, we see a spatially ordered pattern of a seemingly hexagonal symmetry. The existence of such a pattern provides evidence of the interaction between the oscillating filaments, which defines the geometry of the overall structure. We suppose that the neighboring filaments experience a repulsive interaction. When the number of filaments in the device aperture is small, their interaction is not strong enough to organize an ordered structure. As discussed above, solitary filaments seem to be generated stochastically in space. At a high spatial density of pulsating filaments their interaction becomes substantial, which is accompanied by an ordering of filaments in space.

Transverse instabilities of the SGD device for discharge in nitrogen have been investigated theoretically in Refs. [18,20,22]. In these papers, the accumulation of the positive ion charge in the gap, that is, the mechanism related to the transition of discharge to the glow mode, has been found to initiate the formation of patterns. The observation of dynamic patterns at a relatively large current density in our experiments generally supports the main results of the theoretical work. However, it is difficult to make a direct quantitative comparison of the experimental critical current density j_{cr}^2 to that predicted by theory. In this respect, we point out that the systematic theoretical studies of transverse instabilities carried out in Refs. [18,20], as well as the numerical investigations in Ref. [22], dealt only with quasi-one-dimensional SGD systems, that is, the destabilization effects were encountered only in the direction normal to the current.

In our experiments, the estimate of the current density in a filament (these data are extracted from recorded pictures of DSs at short exposure times) yields ≈4 mA/cm^2. So this instantaneous current density exceeds that corresponding to the transition to the glow discharge in the device [25]. (For experimental conditions [N_2, $d_g = 0.84$ mm, and $p = 66$ hPa), the critical current density for the transition is ≈1.4 mA/cm^2.]

Among the characteristic features of glow discharge is the formation of a so-called cathode-fall region in the gap. We attribute to this effect the observed asymmetry of spatial forms of discharge localization at $j > j_{cr}^2$ when changing the polarity of the applied voltage. We point out in this respect that one of the electrodes of the setup is a highly conductive SnO_2 film whose sheet resistance is ≈50 Ω/□. This resistance is several orders of value lower than that of the semiconductor electrode. While the SnO_2 electrode presents an equipotential plane under the conditions of our experiments, the interface between a high-resistivity GaAs electrode and the gas-discharge region does not exemplify such a feature. Therefore, in the case of current filamentation in the gap, neighboring areas of the semiconductor electrode gain different electrical potentials.

When the cathode-fall layer is adjacent to the semiconductor, high tangential electric fields can be generated in the neighborhood of a filament. It is this effect that presumably initiates transversal surface discharges in the form of branching (fractal-like) patterns like that shown in Fig. 5. It is worth noting that similar pictures are observed when studying transient discharges in systems, where at least one of the electrodes is covered by a dielectric. Examples are Lichtenberg figures or patterns at some regimes of operation of dielectric-barrier

discharge devices (see, e.g., [32]). In the case of the present experiments, this effect is expressed when the cathode-fall region of a filament contacts the high-resistance electrode, that is, when the GaAs electrode is under the negative potential.

The theoretical study [18,20] predicts an interesting route of self-organization of a SGD device, where low-amplitude waves running transversally to the current appear as a consequence of the instability. We believe that such an effect does exist in SGD devices for the discharge in nitrogen. However, the sensitivity of the image acquisition technique implemented in the current research is not sufficient to investigate the slightly inhomogeneous distributions of discharge glow for a short exposure time: As noted above, we have been able to obtain the informative snapshots of spatial forms of DSs at small τ_{exp} only for a rather expressed localization of discharge in the gap.

As we have established, irregular spatiotemporal dynamics can be observed in the device at both polarities of applied voltage (see Figs. 5 and 6 and the corresponding discussion in the text). In this respect, it is appropriate to cite recent results [22] where irregular spatiotemporal modes have been presumably revealed in the computational modeling of discharge in a 1D SGD device.

ACKNOWLEDGMENTS

This research was funded by the Russian Foundation for Basic Research (12-02-00889-a). The authors thank Yu. P. Raizer and M. S. Mokrov for helpful discussions. We acknowledge the technical support provided by the company Sedatec, Ltd., which has demonstrated the possibility of applying the camera Phantom v1610 for purposes of the present study.

[1] H.-G. Purwins, H. U. Bödeker, and Sh. Amiranashvili, Dissipative solitons, Adv. Phys. **59**, 485 (2010).

[2] H. Willebrand, C. Radehaus, F.-J. Niedernostheide, R. Dohmen, and H.-G. Purwins, Observation of solitary filaments and spatially periodic patterns in a dc gas-discharge system, Phys. Lett. A **149**, 131 (1990).

[3] H. Willebrand, F.-J. Niedernostheide, E. Ammelt, R. Dohmen, and H.-G. Purwins, Spatio-temporal oscillations during filament splitting in gas discharge systems, Phys. Lett. A **153**, 437 (1991).

[4] C. Radehaus, H. Willebrand, R. Dohmen, F.-J. Niedernostheide, G. Bengel, and H.-G. Purwins, Spatially periodic patterns in a dc gas-discharge system, Phys. Rev. A **45**, 2546 (1992).

[5] H. Willebrand, T. Hünteler, F.-J. Niedernostheide, R. Dohmen, and H.-G. Purwins, Periodic and turbulent behavior of solitary structures in distributed active media, Phys. Rev. A. **45**, 8766 (1992).

[6] A. W. Liehr, *Dissipative Solitons in Reaction Diffusion Systems*, Springer Series in Synergetics (Springer, Berlin, 2013).

[7] C. Strümpel, Yu. A. Astrov, and H.-G. Purwins, Nonlinear interaction of homogeneously oscillating domains in a planar gas discharge system, Phys. Rev. E **62**, 4889 (2000).

[8] C. Strümpel, Yu. A. Astrov, and H.-G. Purwins, Multioscillatory patterns in a hybrid semiconductor gas-discharge system, Phys. Rev. E **65**, 066210 (2002).

[9] C. Strümpel, H.-G. Purwins, and Yu. A. Astrov, Spatiotemporal filamentary patterns in a dc-driven planar gas discharge system, Phys. Rev. E **63**, 026409 (2001).

[10] M. A. Lampert and P. Mark, *Current Injection in Solids* (Academic, New York, 1970).

[11] Yu. A. Astrov, Current structures in Si:Zn, Semiconductors **27**, 1084 (1993) [Phiz. Tekh. Polupr. **27**, 1971 (1993)].

[12] A. Neumann, Slow domains in semi-insulating GaAs, J. Appl. Phys. **90**, 1 (2001).

[13] E. L. Gurevich, Yu. A. Astrov, and H.-G. Purwins, Pattern formation in planar dc-driven semiconductor-gas discharge devices: two mechanisms, J. Phys. D **38**, 468 (2005).

[14] E. L. Gurevich, A. S. Moskalenko, A. L. Zanin, Yu. A. Astrov, and H.-G. Purwins, Rotating waves in a planar dc-driven gas-discharge system with semi-insulating GaAs cathode, Phys. Lett. A **307**, 299 (2003).

[15] Yu. A. Astrov and H.-G. Purwins, Spatiotemporal structures in a transversely extended semiconductor system, Tech. Phys. Lett. **28**, 910 (2002).

[16] E. L. Gurevich, Yu. P. Raizer, and H.-G. Purwins, Self-sustained oscillations in a low-current discharge with a semiconductor serving as a cathode and ballast resistor: I. Experiment, Tech. Phys. **51**, 180 (2006).

[17] Yu. A. Astrov, A. N. Lodygin, and L. M. Portsel, Dynamics and stability of the Townsend discharge in nitrogen in narrow gaps, Phys. Rev. E **89**, 033109 (2014).

[18] D. D. Šijačić, Spatio-temporal pattern formation in a semiconductor-gas-discharge system, Ph.D. thesis, Technische Universiteit Eindhoven, 2004.

[19] D. D. Šijačić, U. Ebert, and I. Rafatov, Oscillations in dc driven barrier discharges: Numerical solutions, stability analysis, and phase diagram, Phys. Rev. E **71**, 066402 (2005).

[20] I. R. Rafatov, D. D. Šijačić, and U. Ebert, Spatiotemporal patterns in a dc semiconductor-gas-discharge system: Stability analysis and full numerical solutions, Phys. Rev. E **76**, 036206 (2007).

[21] Yu. P. Raizer, E. L. Gurevich, and M. S. Mokrov, Self-sustained oscillations in a low-current discharge with a semiconductor serving as a cathode and ballast resistor: II. Theory, Tech. Phys. **51**, 185 (2006).

[22] Yu. P. Raizer and M. S. Mokrov, Physical mechanisms of self-organization and formation of current patterns in gas discharges of the Townsend and glow types, Phys. Plasmas **20**, 101604 (2013).

[23] V. N. Melekhin and N. Yu. Naumov, The dynamic theory of stability of the Townsend discharge and measurement of the critical current, Sov. Phys. Tech. Phys. **29**, 888 (1984) [Zh. Tekh. Fiz. **54**, 1521 (1984)].

[24] A. V. Phelps, Z. Lj. Petrović, and B. M. Jelenković, Oscillations of low-current electrical discharges between parallel-plane electrodes. III. Models, Phys. Rev. E **47**, 2825 (1993).

[25] Yu. P. Raizer, *Gas Discharge Physics* (Springer, Berlin, 1991).

[26] V. Anishchenko, A. Neiman, T. Vadivasova, V. Astakhov, and L. Schimansky-Geier, *Dynamics of Chaotic and Stochastic Systems*, 2nd ed. (Springer, Berlin, 2007).

[27] H. D. I. Abarbanel, R. Brown, J. J. Sidorowich, and L. S. Tsimring, The analysis of observed chaotic data in physical system, Rev. Mod. Phys. **65**, 1331 (1993).

[28] M. Tlidi, K. Staliunas, K. Panajotov, A. G. Vladimirov, and M. G. Clerc, Localized structures in dissipative media: from optics to plant ecology, Philos. Trans. R. Soc. London Ser. A **372**, 20140101 (2014).

[29] The TISEAN software package is publicly available at http://www.mpipks-dresden.mpg.de/∼tisean/.

[30] H. Kantz and T. Schreiber, *Nonlinear Time Series Analysis* (Cambridge University Press, Cambridge, 1997).

[31] M. T. Rosenstein, J. J. Collins, and C. J. De Luca, A practical method for calculating largest Lyapunov exponents from small data sets, Physica D **65**, 117 (1993).

[32] H.-E. Wagner, R. Brandenburg, K. V. Kozlov, A. Sonnenfeld, P. Michel, and J. F. Behnke, The barrier discharge: basic properties and applications to surface treatment, Vacuum **71**, 417 (2003).